LAWRENCE
LIVERMORE
NATIONAL
LABORATORY

LLNL-JRNL-407784

Discrete Properties of Intrinsic Localized Modes Observed in the High Temperature Vibrational Spectrum of NaI

M. E. Manley, A. J. Sievers, J. W. Lynn, S. A. Kiselev, N. I. Agladze, Y. Chen, A. Llobet, A. Alatas

October 14, 2008

Physical Review B

Disclaimer

Discrete Properties of Intrinsic Localized Modes Observed in the High Temperature Vibrational Spectrum of NaI

M. E. Manley[1], A. J. Sievers[2], J. W. Lynn[3], S. A. Kiselev[2], N. I. Agladze[2], Y. Chen[3,4], A. Llobet[5], A. Alatas[6]

[1]*Lawrence Livermore National Laboratory, Livermore, California 94551, USA*
[2]*Laboratory of Atomic and Solid State Physics, Cornell University, Ithaca, New York 14853-2501, USA*
[3]*NIST Center for Neutron Research, National Institute of Standards and Technology, Gaithersburg, Maryland 20899, USA*
[4]*Department of Materials Science and Engineering, University of Maryland, College Park, Maryland 20742, USA*
[5]*Los Alamos National Laboratory, Los Alamos, New Mexico, 87545, USA*
[6]*Argonne National Laboratory, Argonne, Illinois 60439, USA*

Abstract

Inelastic neutron measurements of the high temperature lattice excitations in NaI show surprising features. In thermal equilibrium at 555 K an intrinsic mode, localized in three dimensions, is observed at a single frequency near the center of the spectral phonon gap, polarized along [111]. At higher temperatures mixing between the intrinsic localized mode and the zone boundary TO mode is observed. Higher energy inelastic neutron and x-ray scattering measurements on a room temperature NaI crystal indicate that the creation energy of the ground state of the intrinsic localized mode is 299 meV.

PACS numbers: 63.20.Pw, 63.20.Ry, 78.70.Nx, 63.20.dd

Both classical simulations [1-4] and experiments [4-9] have shown that driving a discrete nonlinear lattice can cause some vibrational energy to spontaneously localize. A long standing question in condensed-matter sciences and nonlinear dynamics is whether or not such intrinsic localized modes (ILMs) can appear in an atomic lattice in thermal equilibrium. Neutron scattering measurements of phonon dispersion curves in solid bcc ^{4}He [10] and in α-U at high temperatures [11,12] have indicated new modes attributed to ILMs, but these interpretations remain speculative since these modes remain within the extended wave spectra and realistic models of the nonlinear lattice dynamics are not available.

Here we report neutron scattering measurements showing an ILM forming in NaI in the spectral phonon gap at 0.594 of the melting temperature. The ILM has a polarization and 3-D localization consistent with classical predictions [13], but, surprisingly, appears with a single frequency, not a distribution. Furthermore, at higher temperatures a mixing between the ILM and the zone boundary TO mode is observed followed by the reappearance of a well defined TO mode. Finally, higher energy inelastic neutron and x-ray scattering measurements on a room temperature NaI crystal display a sharp feature at 299 meV consistent with the creation of a discrete-energy ILM ground state.

Inelastic scattering measurements were performed on a powder of pure NaI and on single crystals of NaI (+0.002Tl). This ionic crystal was chosen since molecular dynamic simulations have already demonstrated that lattice anharmonicity of the two-body potential can stabilize an ILM polarized along [111] in the phonon gap of a 3-D diatomic crystal with rigid ion NaI potentials [13], and since it had been proposed that at

high temperatures such ILMs may appear in the gap, stabilized by configurational entropy, much like vacancies only with much lower activation energy [14].

The pure NaI powder was measured on the LANSCE-PHAROS time-of-flight chopper spectrometer at Los Alamos National Laboratory from room temperature to 555 K. The incident energy was 45 meV and the detector coverage (7º to 140º) gave momentum transfers spanning several Brillouin Zones. The raw data were corrected for sample environment background, detector efficiency and the k_i/k_f phase space factor. A neutron-cross-section weighted phonon density of states was extracted from the results by subtracting the elastic peak, the incoherent multiphonon scattering determined iteratively [15, 16], and dividing out the thermal occupation and Debye-Waller factors. Figure 1 shows the resulting temperature-dependent phonon densities of states (DOS). In addition to the expected uniform softening of all the phonon peaks with increasing temperature there are several interesting features. First, a new peak accounting for about 0.0082 of the DOS develops near the middle of the gap (around 10.5 meV at 555 K). Second, the TO mode, appearing at room temperature as a strong peak around 14.5 meV, decreases in relative intensity with increasing temperature.

To obtain specific spectral information single crystals of NaI (+0.002Tl) [17] were measured using the bt7 triple-axis spectrometer at the NIST Center for Neutron Research. The spectrometer was operated with fixed final neutron energy of 14.7 meV and the crystals were mounted in a furnace with the (*hhl*) reflections in the scattering plane. Figure 2 shows the temperature dependence of energy scans in a nearly transverse geometry along [111] at the zone boundary (ZB). At room temperature, the ZB TA, ZB LA, and ZB TO modes are all visible and have energies consistent with those reported

previously [18-21]. On heating to 555 K, a new peak again appears in the gap, refining to a position at 10 meV. The intensity of this feature in this scattering geometry indicates a strong component of polarization along [111]. At a temperature of 473 K, just below where the gap mode is evident, some intensity is lost in the ZB TO mode. The center frequencies of the ZB TA and ZB LA mode decrease with increasing temperature as expected for a thermally expanding lattice; however, the ZB TO mode frequency remains fixed near 12.8 meV between 438 and 555 K.

Using a longitudinal scattering geometry with $\boldsymbol{Q}$ = (2.5, 2.5, 2.5) the temperature dependence of different modes was measured over a wider temperature range as shown in Fig. 3. With the experimental uncertainty of ±0.2 meV the LA mode position with increasing temperature is: 9.7 meV, 300K; 8.7 meV, 555 K; 8.6 meV, 660 K; 8.3 meV, 768 K. The gap mode at 555 K now appears as a significant shoulder at 10.3 meV on the more prominent ZB LA mode. The ZB TO mode shows unusual behavior in the temperature interval above 555 K. At 660 K the ILM and ZB TO form a broad mix then at 768 K a well defined single mode reappears that shows positive dispersion moving in from the ZB.

Additional measurements on dispersion properties at 555 K are summarized in Fig. 4(a). The gap mode stands out as dispersionless across the zone, with weakening intensity towards the zone center; in addition, there is no clear indication of transverse or longitudinal character for this mode. The LA mode softening with increased temperature is focused near the zone boundary, while the softening in the TO and TA branches is more uniform.

The ***Q*** dependence (structure factor) of the gap mode intensity was determined from constant-energy ***Q*** scans performed across the zone near (222). Between 9 meV and 12 meV evidence of three features appear above background as shown in Fig. 4(b). Top panel: At 12 meV the ***Q*** dependence is relatively flat, decreasing slightly towards the zone center, consistent with the measured TO mode dispersing slightly upward towards the zone center. Center panel: At 10 meV where the gap mode is dominant, the intensity appears smoothly spread across ~1/3 of the zone in a Gaussian shape centered at the zone boundary and fading to background near the zone center. Bottom panel: At 9 meV the gap mode intensity overlaps with the LA modes, which peak in energy near q = (0.38, 0.38, 0.38), see the LA mode dispersion in Fig. 4(a). Taken together with the dispersion curve data, it is clear that the Gaussian structure observed in the 10 meV scan is a fair representation of the gap mode structure factor. Since a Gaussian feature in reciprocal space transforms to a Gaussian feature in real space with inverse width, the local mode structure factor implies a Gaussian shaped mode about 1.2 nm across.

Since recent inelastic scattering work in uranium indicated a second much higher energy lattice excitation [12], higher energy inelastic neutron and inelastic x-ray scattering measurements have also been performed on single crystals of NaI(+0.002Tl) at room temperature. The neutron measurements used 441 meV neutrons in the LANSCE-PHAROS time-of-flight chopper spectrometer located at Los Alamos National Laboratory. The crystal was oriented so that the dominant direction of the ***Q*** vector was along the [111] direction in the (*hhl*) plane. The resulting spectra were selectively summed over regions in ***Q***-space that were either near zone boundaries, where the gap mode appears strong, or near zone centers, where the gap mode intensity is absent,

illustrated in Fig. 4(a,b). The resulting spectra summed near the zone boundaries are shown in the top panel of Fig. 5(a). Evident is a series of three or four broad spectral features ending with a fairly sharp excitation at 299 meV. By contrast, the sum near the zone center displays a featureless spectrum, bottom panel in Fig. 5(a). The sharp 299 meV zone boundary feature was also observed with inelastic x-ray scattering using the 3IDC-C spectrometer at the Advanced Photon Source of Argonne National Laboratory with incident x-ray energy of 21.657 keV. Figure 5(b) displays a weak excitation at 298 meV at the zone boundary while no excitations are observed near the zone center.

Six remarkable ILM signatures appear in these inelastic scattering data on NaI. (1) The sharp spectral feature in the gap at 555 K (Figs. 1-3) in both powder and single crystals; (2) The absence of dispersion for the gap mode [Fig. 4(a)], its intensity distribution in $\boldsymbol{Q}$-space [Fig. 4(b)], and its [111] polarization [Fig. 3]; (3) The temperature independence of the ZB TO mode between 438 and 555 K [some data shown in Figs. 2,3]; (4) The mixed dynamical ILM-TO spectrum in the gap at 660 K (Fig. 3); (5) The sharp ZB TO mode observed at 768K; and (6) The 299 meV (Fig. 5) peak observed both with INS and IXS.

Our interpretations of these numbered items are as follows: (1) The peak in the phonon gap demonstrates that a thermally activated ILM has a single vibrational frequency, not a distribution. (2) These three features are consistent with earlier molecular dynamics predictions in NaI of the ILM orientation and structure [13]. (3) From the temperature dependence of the ZB TO mode between 300 K and 765 K shown in Fig. 3 the same mode shown in Fig. 2 should have decreased by 0.9 meV between 438 and 555 K. Since it appears temperature independent over this interval, we propose that

some thermal energy with increasing temperature goes into producing more ILMs rather than increasing the ZB TO amplitude and lowering its frequency. The associated lattice thermal expansion may also manifest through ILM production since each is accompanied by a localized dc distortion that provides a localized thermal expansion for the lattice [13]. (4) At this higher temperature the ILM concentration is sufficiently large that ILMs and the ZB TO mode interact. (5) With a diatomic 1-D model it has been shown that the ZB TO mode decreases in frequency with increasing amplitude faster than does the associated ILM [22]; hence, we propose that this temperature is where islands of extended ILM waves and the ZB TO mode become indistinguishable. Now all ions in the resulting excitation have the new larger (ILM) vibrational amplitude resulting in an extended wave ZB TO mode, albeit at a lower frequency. (6) Identifies the creation energy of the ground state of an ILM. Although requiring a large energy (~21 phonons), these localized excitations become visible at high temperatures because of configurational entropy. To provide maximum entropy these ILMs only occur at a single frequency near the center of the gap, insuring the smallest possible spatial extent. Our findings demonstrate that localized vibrational excitations with well-defined discrete energies are a new, necessary component to understand the high-temperature lattice dynamics of crystalline solids.

Acknowledgments

Work performed under the auspices of the U.S. Department of Energy by Lawrence Livermore National Laboratory under Contract DE-AC52-07NA27344. Cornell effort supported by DOE DE-FG02-04ER46154. AJS would like to thank S. P. Love, J. B. Page and J. P. Sethna for helpful comments. The use of the Advanced Photon Source was

supported by the Department of Energy, Office of Science, Office of Basic Energy Sciences, under Contract No. DE-ACOZ-06CH11357.

References

[1] B. A. Malomed, Phys. Rev. A **45**, 4097 (1992).

[2] T. Rössler and J. B. Page, Phys. Rev. B **62**, 11460 (2000).

[3] D. K. Campbell, S. Flach, and Y. S. Kivshar, Physics Today **57**, 43 (2004).

[4] S. Flach and A. Gorbach, *Discrete breathers-Advances in theory and applications* (Elsevier Science, 2008).

[5] W.-Z. Chen, Phys. Rev. B **49**, 15063 (1994).

[6] P. Marquie, J. M. Bilbault, and M. Remoissenet, Phys. Rev. E **51**, 6127 (1995).

[7] U. T. Schwarz, L. Q. English, and A. J. Sievers, Phys. Rev. Lett. **83**, 223 (1999).

[8] M. Sato, B. E. Hubbard, A. J. Sievers, B. Ilic, D. A. Czaplewski, and H. G. Craighead, Phys. Rev. Lett. **90**, 044102 (2003).

[9] M. Sato and A. J. Sievers, Nature **432**, 486 (2004).

[10] T. Markovich, E. Polturak, J. Bossy, and E. Farhi, Phys. Rev. Lett. **88**, 195301 (2002).

[11] M. E. Manley, M. Yethiraj, H. Sinn, H. M. Volz, J. C. Lashley, W. L. Hults, G. H. Lander, and J. L. Smith, Phys. Rev. Lett. **96**, 125501 (2006).

[12] M. E. Manley, A. Alatas, F. Trouw, B. M. Leu, J. W. Lynn, Y. Chen, and W. L. Hults, Phys. Rev. B **77**, 214305 (2008).

[13] S. A. Kiselev and A. J. Sievers, Phys. Rev. B **55**, 5755 (1997).

[14] A. J. Sievers and S. Takeno, Phys. Rev. Lett. **61**, 970 (1988).

[15] G. L. Squires, *Introduction to the Theory of Neutron Scattetring* (Cambridge University Press, Cambridge, 1978).

[16] M. E. Manley, R. J. McQueeney, B. Fultz, R. Osborn, G. H. Kwei, and P. D. Bogdanoff, Phys. Rev. B **65**, 144111 (2002).

[17] The inelastic scattering intensity from the Tl contributes less than 0.00055 relative to the NaI and can therefore be ignored.

[18] G. O. Jones, D. H. Martin, P. A. Mawer, and C. H. Perry, Proc. Roy. Soc. (London) Math. & Phys. Sciences **261**, 10 (1961).

[19] A. B. D. Woods, B. N. Brockhouse, R. A. Cowley, and W. Cochran, Phys, Rev. **131**, 1025 (1963).

[20] J. S. Melvin, J. D. Pirie, and T. Smith, Phys. Rev. **173**, 1082 (1968).

[21] D. B. Sirdeshmukh, L. Sirdeshmukh, and K. G. Subhadra, *Alkali Halides: A handbook of Physical Properties*, edited by A. Zunger, R.M. Osgood, H. R, and H. Sakaki, Materials Science (Springer-Verlag, Berlin, 2002).

[22] D. Bonart, T. Rössler, and J. B. Page, Phys. Rev. B **55**, 8829 (1997). See Fig. 5, curves a' and b'.

Figure captions

Figure 1. Neutron-weighted phonon density of states (DOS) measured on pure NaI powder at 310, 400, 500, and 555 K. A relatively sharp feature appears near the center of the phonon gap at the highest temperature.

Figure 2. Inelastic-neutron-scattering spectra measured along [111] at the zone boundary of a NaI crystal in a nearly-transverse-scattering geometry (geometry shown in inset). Fits are made to multiple peaks, including the transverse acoustic (TA), longitudinal acoustic (LA), transverse optic (TO), and the ILM peak, appearing at 555 K and 10 meV.

Figure 3. Inelastic-neutron-scattering spectra measured along [111] at the zone boundary of a NaI crystal in longitudinal geometry (geometry shown in inset). The high temperature data are offset for clarity. Fits are made to the LA and TO peaks at most temperatures. The incoherent multiphonon scattering background has been subtracted from the data collected at 555 K and above. The new peak at 10.3 meV at 555 K is consistent with the feature in Figs 1 and 2. At 660 K a more complex spectra is evident followed by the single TO mode at 768 K.

Figure 4. Summary of lattice dynamics measured in NaI along the [111] direction. **a,** Phonon dispersion curves at 90 K (dashed) from Ref. 19 and 555 K (solid) from this work, including a dispersionless local mode that appears in the gap. **b,** Constant-energy $\boldsymbol{Q}$ scans at 545 K measured in a transverse geometry (geometry shown in inset). Data from scans away from the phonons at 20 meV, shown in all scans, gives a measure of the background. The intensity at 10 meV, middle panel, is fit to a Gaussian. Intensities associated with the TO mode (top panel) and LA mode (bottom panel) are also indicated, see text.

Figure 5. High-energy inelastic lattice response along [111] for a room temperature NaI crystal probed using neutron and x-ray scattering. **a,** Inelastic neutron scattering (INS) using 441 meV neutrons on the PHAROS-LANSCE spectrometer summed near zone boundaries (top panel), and near zone centers (bottom panel). The harmonic multiphonon contribution, which cuts off around 140 meV, was calculated in the incoherent approximation using the measured room temperature phonon density of states (Fig. 1). **b,** Reciprocal space sampled by the PHAROS spectrometer. Here a neutron energy loss of 299 meV is assumed and this cut in Q space is illustrated, along with the regions near and away from the zone boundaries as applied in the detector sums. **(c)** Inelastic x-ray scattering (IXS) collected near the 299 meV peak on the zone boundary (top panel) and near the zone center (bottom panel).

Figures

Figure 1

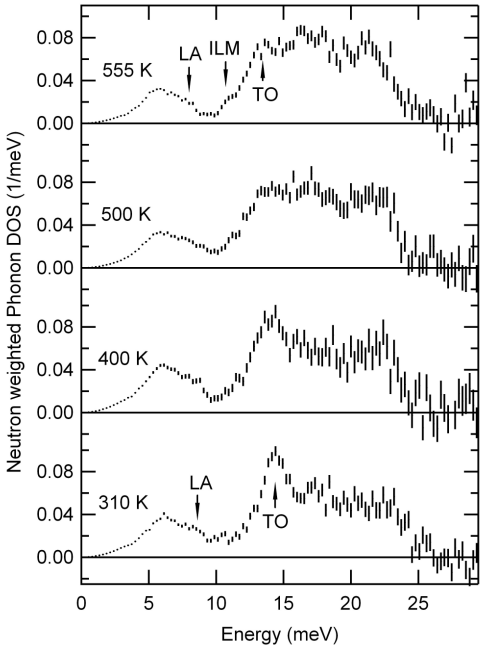

Figure 2

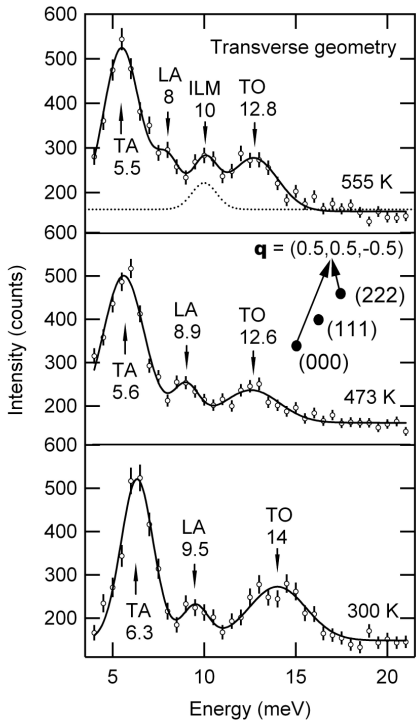
Transverse geometry
LA
8
ILM
10
TO
12.8
TA
5.5
555 K
q = (0.5,0.5,-0.5)
(222)
(111)
(000)
LA
8.9
TO
12.6
TA
5.6
473 K
LA
9.5
TO
14
TA
6.3
300 K
Intensity (counts)
Energy (meV)

Figure 3

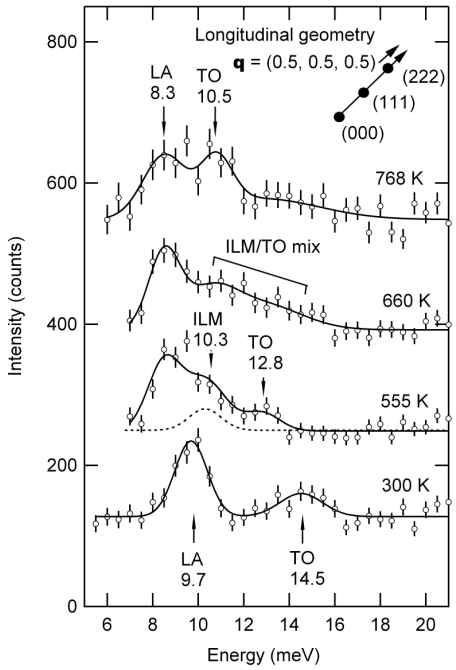
Longitudinal geometry
q = (0.5, 0.5, 0.5)
(222)
(111)
(000)
LA
8.3
TO
10.5
768 K
ILM/TO mix
660 K
ILM
10.3
TO
12.8
555 K
300 K
LA
9.7
TO
14.5
Intensity (counts)
Energy (meV)
0
200
400
600
800
6
8
10
12
14
16
18
20

Figure 4

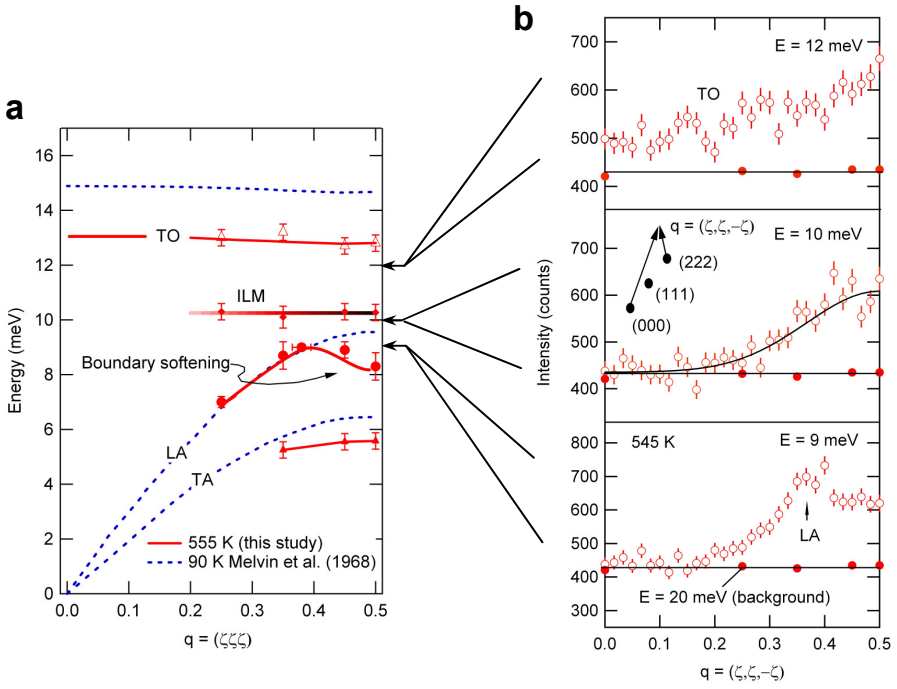
a
b
Energy (meV)
q = (ζζζ)
TO
ILM
Boundary softening
LA
TA
555 K (this study)
90 K Melvin et al. (1968)
Intensity (counts)
E = 12 meV
TO
E = 10 meV
q = (ζ,ζ,−ζ)
(222)
(111)
(000)
545 K
E = 9 meV
LA
E = 20 meV (background)
q = (ζ,ζ,−ζ)

Figure 5

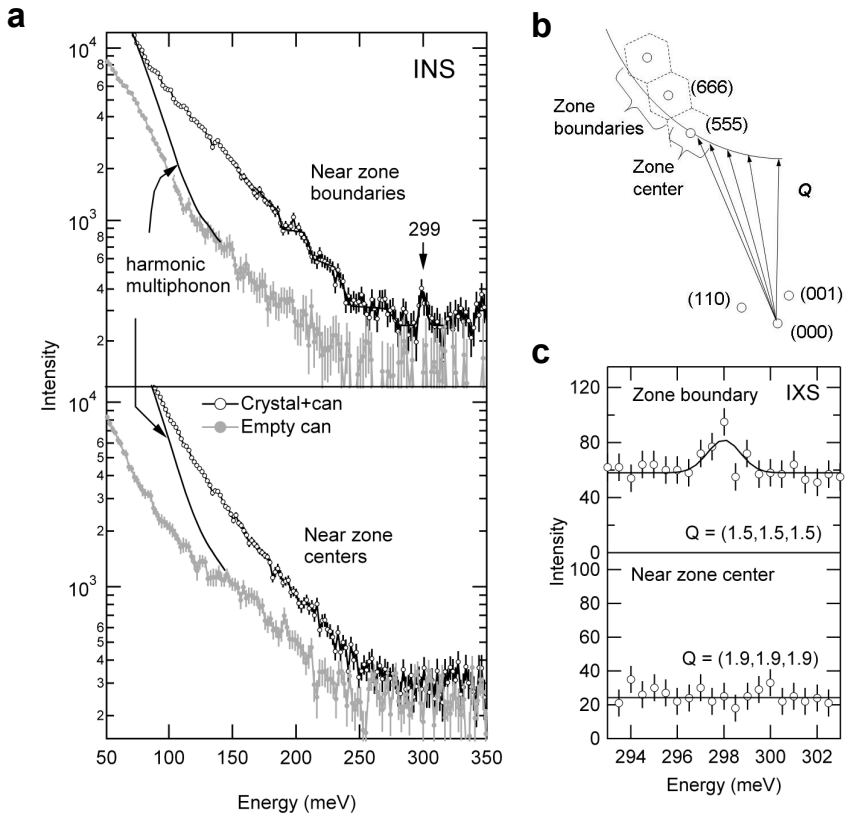
a
INS
Near zone boundaries
299
harmonic multiphonon
Crystal+can
Empty can
Near zone centers
Intensity
Energy (meV)
b
Zone boundaries
(666)
(555)
Zone center
Q
(110)
(001)
(000)
c
Zone boundary
IXS
Q = (1.5,1.5,1.5)
Near zone center
Q = (1.9,1.9,1.9)
Intensity
Energy (meV)